Trans. Phenom. Nano Micro Scales, 3(1): 37-45, Winter - Spring 2015
DOI: 10.7508/tpnms.2015.01.004

ORIGINAL RESEARCH PAPER

MHD Natural Convection and Entropy Generation of Variable Properties Nanofluid in a Triangular Enclosure

A. Aghaei[1,*], G.A. Sheikhzadeh[1], H.R. Ehteram[1], M. Hajiahmadi[1]
[1]Mechanical engineering Department, university of Kashan, Kashan, I.R. Iran

ARTICLE INFO.

Article history
Received 16 May 2014
Accepted 7 January 2015

Keywords
Bejan Number
Brownian Motion
Entropy Generation
Hartman Number
Nanofluid
Triangular Enclosure

Abstract

Natural convection heat transfer has many applications in different fields of industry; such as cooling industries, electronic transformer devices and ventilation equipment; due to simple process, economic advantage, low noise and renewed retrieval. Recently, heat transfer of nanofluids have been considered because of higher thermal conductivity coefficient compared with those of ordinary fluids. In this study; natural convection and entropy generation in a triangular enclosure filled by Al_2O_3 –water nanofluid affected by magnetic field considering Brownian motion is investigated numerically. Two inclined walls are maintained at constant cold temperature (T_c) while the bottom wall is kept at constant high temperature (T_h) with (T_h>T_c). In order to investigate natural convection, a computer program (FORTRAN language) based on finite volume method and SIMPLER algorithm has been used. Analyses is performed for volume fraction of nanoparticles 0, 0.02, 0.04, Hartmann number 0, 50,100, Rayleigh numbers 10^3,10^4,10^5 and angle of inclined walls 45^0. In investigated angles and Rayleigh numbers; average Nusselt number is increased by enhancement of volume fraction of nanoparticles in a fixed Hartmann number. It is also observed that total entropy generation variations by increasing volume fraction of nanoparticles are similar to that of Nusselt number. By the results; effect of friction is always insignificant on generated entropy. It is observed that natural convection of nanofluid is decreased by enhancement of Hartmann number and its behavior is close to thermal conduction. It is also concluded that average Nusselt number and total generated entropy are decreased.

1. Introduction

Natural convection heat transfer has many applications in different fields of industry such as cooling industries, electronic transformer devices and ventilation equipment; due to simple process, economic advantage, low noise and renewed retrieval. Because of higher thermal conductivity, Heat transfer of nanofluids has been considered recently compared with ordinary fluids.

*Corresponding author
Email address: AlirezaAghaei21@gmail.com

Nomenclature

B	Magnetic field		**Greek Symbols**
c_P	Specific heat (Jkg-1K-1)	α	Thermal diffusivity coefficient (m2s-1)
d_f	Diameter of water molecule (nm)	β	Thermal expansion coefficient(K-1)
d_p	Diameter of nanoparticle (nm)	μ	viscosity (kgm-2s-1)
L	Height of the enclosure (m)	υ	Kinematic viscosity(m2s-1)
Ha	Hartmann number	θ	Dimensionless temperature
k	Thermal conductivity (Wm-1K-1)	ρ	density (kgm-3)
p	pressure (pa)	φ	Volume fraction of nanoparticles
P_r	Prandtl number		**Subscripts**
R_a	Rayleigh number	Avg	average
s	Entropy	c	cold
S_{mf}	Entropy generation of magnetic field (≈0)	f	fluid
T	Temperature (K)	h	hot
T_H	Temperature of the hot wall (K)	nf	nanofluid
T_c	Temperature of the cold wall (K)	p	particle

Ghasemi and Aminossadati [1] investigated mixed convection of Al_2o_3-Water nanofluid in a right angle triangular enclosure. Based on their results, heat transfer increases with increasing the volume fraction of nanoparticles.

Ho et al. [2] performed a numerical study to investigate free convection heat transfer of Al_2o_3-water in a square enclosure by finite volume method. They found that different models of viscosity lead to predict various values of Nusselt number. Oztop and Abu-Nada [3] analyzed the fluid flow and heat transfer due to natural convection in a heated cavity. Their results showed that using nanofluid in low aspect ratio cavities make higher enhancement in heat transfer. Mahmoodi and Hashemi [4] investigated natural convection heat transfer and fluid flow of Cu-Water nanofluid in a c-shape enclosure. They observed that average Nusselt number increased with increasing Rayleigh number and volume fraction of nanoparticles. Because the entropy generation is a measure of destruction of available work of the system, determination of entropy generation is important to enhance system efficiency, Bejan [5]. Recently, entropy generation minimization has been considered a lot to reach optimum design of systems, Mahian et al. [6].

Dagtekin et al. [7], investigated numerically the entropy generation in natural convection fluid flow in Γ-shape enclosure. Their results showed that entropy generation duo to heat transfer is the main part of total entropy. Ilis et al. [8]carried out a numerical work to investigate influence of aspect ratio on entropy generation for natural convection fluid flow in rectangular enclosures. They observed that by increasing aspect ratio the entropy generation increases up to a maximum value and then decreases. Varol et al. [9] performed a numerical study to analyze the natural convection and entropy generation. Based on their results with decreasing Rayleigh number, Bejan number that is defined as the ratio of generated entropy due to heat transfer to the total entropy generation, decreases.

One considerable point in study of convective heat transfer is disagreement between the experimental results, Abbasian et al. [10] and [11], and numerical studies for nanofluids. Maybe one reason for this disconformity is to ignore some phenomenon like Brownian motion. In Brownian motion, fluid molecules are constantly hitting nanoparticles and disperse them inside the fluid. In present study the effect of this phenomenon is considered. Through a comprehensive investigation it is observed that few studies has been done on entropy generation of nanofluid with various properties in triangular enclosures.

Novelty of this article is investigation magnetic field effect on triangular enclosure, entropy generation, using the variable properties for viscosity and thermal conductivity coefficient estimation, and Brownian motion of nanoparticles effect. This simulation can be a model of cooling an electronic device (for example at computer boards). At present study influence of fluid flow, heat transfer and entropy generation is investigated in natural convection of Al_2O_3-Water nanofluid in a triangular enclosure with hot bottom wall and cold sidewalls for various Rayleigh numbers, Hartmann numbers and volume fraction of nanoparticles and at θ_s=45°.

2.Governing equations and boundary conditions

Schematic view of the problem and its boundary conditions is shown in figure 1.

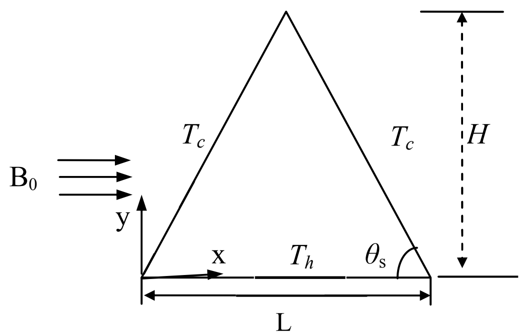

Fig. 1. schematic view of the enclosure with boundary conditions

The bottom wall is kept at hot temperature (T_H) and sidewalls are maintained at cold temperature (T_c). All the walls are assumed to be electrically insolated. Study is done for the Rayleigh numbers of 10^3,10^4,10^5, Hartmann numbers of 0, 50,100, angle of inclined sidewalls with horizon 45° and nanoparticles' volume fraction of 0-0.04. The height of the enclosure, H is presumed to be constant.

The value of θ_s is θ_s=45°. Thermophysical properties of water as the base fluid and Al_2O_3 nanoparticles are presented in table 1 Abu-Nada et al. [12].

Table 1
Thermophysical properties of base fluid and the nanoparticles, Abu-Nada et al. [12].

	β **(K^{-1})**	***k*** **($Wm^{-1}K^{-1}$)**	***c_p*** **($jkg^{-1}K^{-1}$)**	***ρ*** **(kgm^{-3})**
water	2.1×10^{-4}	0.613	4179	997.1
Al_2O_3	0.85×10^{-5}	25	765	3970

The influence of magnetic field as Lorentz volumetric force is taken into account in momentum equation in term of $\vec{F} = \vec{J} \times \vec{B}$ where $\vec{B}$ is magnitude of magnetic field and $\vec{J}$ is density of electrical flow. The continuity equation, entropy generation and stream function affected by magnetic field are given by:

$$\frac{\partial u}{\partial x} + \frac{\partial v}{\partial y} = 0 \tag{1}$$

$$u\frac{\partial u}{\partial x} + v\frac{\partial u}{\partial y} = -\frac{1}{\rho_{nf}}\frac{\partial p}{\partial x} + \frac{1}{\rho_{nf}}[\frac{\partial}{\partial x}(\frac{\mu_{nf}\partial u}{\partial x}) + \frac{\partial}{\partial y}(\frac{\mu_{nf}\partial u}{\partial y})] + \sigma_{nf}B_0^2\left(v\cos\phi\sin\phi - u\sin^2\phi\right) \tag{2}$$

$$u\frac{\partial v}{\partial x} + v\frac{\partial v}{\partial y} = -\frac{1}{\rho_{nf}}\frac{\partial p}{\partial y} + \frac{1}{\rho_{nf}}[\frac{\partial}{\partial x}(\frac{\mu_{nf}\partial v}{\partial x}) + \frac{\partial}{\partial y}(\frac{\mu_{nf}\partial v}{\partial y})] + \frac{(\rho\beta)_{nf}}{\rho_{nf}}g(T - T_c) + \sigma_{nf}B_0^2\left(u\cos\phi\sin\phi - v\cos^2\phi\right) \tag{3}$$

$$u\frac{\partial T}{\partial x} + v\frac{\partial T}{\partial y} = -\frac{1}{(\rho c_p)_{nf}}[\frac{\partial}{\partial x}(\frac{k_{nf}\partial T}{\partial x}) + \frac{\partial}{\partial y}(\frac{k_{nf}\partial T}{\partial y})] \tag{4}$$

$$S_{gen} = \frac{k_{nf}}{T_0^2}\left[\left(\frac{\partial T}{\partial x}\right)^2 + \left(\frac{\partial T}{\partial y}\right)^2\right] + \frac{\mu_{nf}}{T_0}[2\left(\frac{\partial u}{\partial x}\right)^2 + 2\left(\frac{\partial v}{\partial y}\right)^2 + \left(\frac{\partial u}{\partial y} + \frac{\partial v}{\partial x}\right)^2] + s_{mf} \tag{5}$$

$$\psi(x, y) = \int u\,dy + \psi_0 \tag{6}$$

By employing dimensionless variables and considering horizontal magnetic field in the x-direction, dimensionless equations of continuity, momentum, energy conservation and entropy generation are obtained from 2-6.

$$X = \frac{x}{L}, Y = \frac{y}{L}, U = \frac{uL}{\alpha_f}, V = \frac{vL}{\alpha_f}, P = \frac{pL^2}{\rho_{nf}\alpha_f^{\ 2}}$$

$$\theta = \frac{T - T_c}{T_h - T_c}, T_0 = \frac{T_h + T_c}{2}, \Delta T = T_h - T_c, \tag{7}$$

$$\mathrm{Ra} = \frac{g\beta\Delta T L^3}{\nu\alpha},\ \mathrm{Ha} = B_0 H\sqrt{\frac{\sigma_{nf}}{\rho_{nf}\upsilon_f}}$$

Subtitles of f and n_f, represent base fluid and nanofluid, respectively.

$$\frac{\partial U}{\partial X}+\frac{\partial V}{\partial Y}=0 \tag{8}$$

$$U\frac{\partial U}{\partial X}+V\frac{\partial U}{\partial Y}=-\frac{\partial P}{\partial X}+\frac{1}{\rho_{nf}\alpha_f}\frac{\partial}{\partial X}\left(\mu_{nf}\frac{\partial U}{\partial X}\right)+\frac{\partial}{\partial Y}\left(\mu_{nf}\frac{\partial U}{\partial Y}\right) \tag{9}$$

$$U\frac{\partial V}{\partial X}+V\frac{\partial V}{\partial Y}=-\frac{\partial P}{\partial Y}+\frac{1}{\rho_{nf}\alpha_f}[\frac{\partial}{\partial X}\left(\mu_{nf}\frac{\partial U}{\partial X}\right)+\frac{\partial}{\partial Y}\left(\mu_{nf}\frac{\partial U}{\partial Y}\right)]+\frac{(\rho\beta)_{nf}}{\rho_{nf}\beta_f}Ra\Pr\theta-\mathrm{Ha}^2\times\mathrm{Pr}\times V\cos\phi \tag{10}$$

$$U\frac{\partial \theta}{\partial X}+V\frac{\partial \theta}{\partial Y}=\frac{1}{(\rho c_p)_{nf}\alpha_f}[\frac{\partial}{\partial X}\left(k_{nf}\frac{\partial \theta}{\partial X}\right)+\frac{\partial}{\partial Y}\left(k_{nf}\frac{\partial \theta}{\partial Y}\right)] \tag{11}$$

Dimensionless stream function is defined as follows:

$$\Psi(X,Y)=\int U\,dY+\Psi_0 \tag{12}$$

Total entropy generation that includes both of entropy due to heat transfer and entropy due to fluid friction is obtained by this relation, Bejan [13]:

$$S'''_{gen}=\frac{k_{nf}}{k_f}\left[\left(\frac{\partial\theta}{\partial X}\right)^2+\left(\frac{\partial\theta}{\partial Y}\right)^2\right]+\chi\frac{\mu_{nf}}{\mu_f}\left[\begin{array}{l}2\left(\frac{\partial U}{\partial X}\right)^2+\\ 2\left(\frac{\partial V}{\partial Y}\right)^2+\left(\frac{\partial U}{\partial Y}+\frac{\partial V}{\partial X}\right)^2\end{array}\right]+S_{mf} \tag{13}$$

$$\chi=\frac{\mu_{nf}T_0}{k_f}\left(\frac{\alpha_f}{L\,\Delta T}\right)^2$$

Dimensionless boundary conditions are given by:

$$\begin{array}{l}U=V=0,\ \theta=0\text{, On the sidewalls of enclosure}\\ U=0, V=0,\ \theta=1\text{, On the hot side}\end{array} \tag{14}$$

Nanofluid properties such as; density, heat capacity, thermal expansion coefficient, thermal diffusivity coefficient, static viscosity, Brinkman [14], and static thermal conductivity coefficient, Maxwell [15], are obtained by 15-24 relations, respectively:

$$\rho_{nf}=(1-\varphi)\rho_f+\varphi\rho_s \tag{15}$$

$$(\rho c_p)_{nf}=(1-\varphi)(\rho c_p)_f+\varphi(\rho c_p)_s \tag{16}$$

$$(\rho\beta)_{nf}=(1-\varphi)(\rho\beta)_f+\varphi(\rho\beta)_s \tag{17}$$

$$\alpha_{nf}=\frac{k_{nf}}{(\rho c_p)} \tag{18}$$

$$\mu_{Static}=\mu_f(1-\varphi)^{-2.5} \tag{19}$$

$$k_{Static}=k_f\left[\frac{(k_s+2k_f)-2\varphi(k_f-k_s)}{(k_s+2k_f)+\varphi(k_f-k_s)}\right] \tag{20}$$

$$\mu_{eff}=\mu_{Static}+\mu_{Brownian} \tag{21}$$

$$k_{eff}=k_{Static}+k_{Brownian} \tag{22}$$

Where $\mu_{Brownion}$ and $k_{Brownion}$ are, Koo [16]:

$$\mu_{Brownian}=5\times10^4\varphi\rho_f\sqrt{\frac{\kappa T}{2\rho_s R_s}}\xi(T,\varphi) \tag{23}$$

$$k_{Brownian}=5\times10^4\varphi\rho_f c_{p,f}\sqrt{\frac{\kappa T}{2\rho_s R_s}}\xi(T,\varphi) \tag{24}$$

Influence of Brownian motion in terms of temperature is observed at viscosity (23) and thermal conductivity coefficient (24) (Viscosity and thermal conductivity coefficient change with temperature). ρ_s and R_s are density and radius of nanoparticles (23.5×10^{-9}), respectively and κ is the Boltzmann constant ($K=1.3807\times10^{-23}$(J/k)).

For Al_2o_3-Water nanofluid function ζ that is estimated experimentally is defined as, Li [17]:

$$\begin{array}{l}\zeta=[a+b\ln(dp)+c\ln(\varphi)+d\ln(\varphi)\ln(dp)+b\ln(dp)^2]\\ \ln(T)+(g+h\ln(dp)+i\ln(\varphi)+j\ln(\varphi)\ln(dp)+k\ln(dp)^2)\end{array} \tag{25}$$

Constants of equation (19) for Al_2o_3-Water is shown at table 2, Li [17].

Table 2
Li [17], Constants of relation (19).

constant	amount	constant	amount
a	52.8135	g	-298.1981
b	6.1156	h	-34.5327
c	0.6956	i	-3.92253
d	0.0417	j	-0.2354
e	0.1769	k	-0.9991

Convection heat transfer coefficient is:

$$h_{nf} = \frac{q}{T_h - T_c} \tag{26}$$

Nusselt number that it characteristic length measured by the height of the enclosure is:

$$\mathrm{Nu} = \frac{h_{nf} H}{k_f} \tag{27}$$

Heat flux per unit area is given by:

$$q = -k_{nf} \frac{T_h - T_c}{H} \left.\frac{\partial \theta}{\partial Y}\right|_{Y=0} \tag{28}$$

Substituting relations (26) and (28) in (27), gives the Nusselt number:

$$\mathrm{Nu} = -\left(\frac{k_{nf}}{k_f}\right) \left.\frac{\partial \theta}{\partial Y}\right|_{Y=0} \tag{29}$$

The average Nusselt number on the hot wall is:

$$\mathrm{Nu}_{\mathrm{Avg}} = \frac{1}{L}\int_0^1 Nu\, dX \tag{30}$$

3. Numerical implementation

Governing equations by using the finite volume method and SIMPLER algorithm and computer program (FORTRAN language) are solved numerically.

In order to validate the results of the computer program, the numerical simulation of reference, Oztop and Abu-Nada [3], was used.

The results of this simulation is compared with the results of Oztop and Abu-Nada [3], and is given at table 3.

Table 3
Comparisons of the present results for average Nusselt number With the results of Oztop and Abu-Nada [3].

Ra	ψ	Present study	amount
10^3	0.00	1.008	1.004
	0.05	1.119	1.122
10^5	0.00	3.993	3.983
	0.05	4.234	4.271

In order to determine a proper grid for the numerical simulation, a grid study is conducted for the Al_2o_3-Water nanofluid, average Nusselt numbers from the different uniform grids are presented in table 4. It is observed from the results that a 111×61uniform grid is sufficiently fine to ensure a grid independent solution. Hence, this grid is used to perform all subsequent calculations.

Table 4
Average Nusselt number at the walls of the enclosure for Al_2o_3-Water nanofluid at $\theta_s=45^\circ$, $Ra=10^5$, $\varphi=0.04$.

Number of Nodes	Nu_{avg}
71×41	12.06
91×51	12.34
111×61	12.48
131×71	12.50
151×81	12.51
171×91	12.51

The convergence criterion for pressure, temperature and velocity is obtained from following relation Where m and n are the number of grid points in x- and y- direction, respectively, ζ is any of the computed field variables, k is the iteration number.

$$\mathrm{Error} = \frac{\sum_{i=1}^{M}\sum_{j=1}^{N}\left|\zeta_{i,j}^{k+1} - \zeta_{i,j}^{k}\right|}{\sum_{i=1}^{M}\sum_{j=1}^{N}\left|\zeta_{i,j}^{k+1}\right|} \le 10^{-6} \tag{31}$$

4. Results and discussions

Figure 2 shows the streamlines, isotherms and total entropy generation at different Rayleigh and Hartmann numbers.

For a constant Rayleigh number, with increasing Hartmann number, the eyes of the eddies tend toward the bottom vertices of the triangular enclosure. This is because of the Lorentz force due to magnetic field which prevents natuaral convection of nanofluid and its moving in vetical direction of the enclosure. For a constant Hartmann number, with increasing Rayleigh number, eddies tend toward the center of the enclosure and stretch in vertical direction and become more powerfull. For Rayleigh number(=10^3) and all investigated Hartmann numbers, streamlines have slight curves which shows that natural convection of nanofluid is weak.

At Ra =10^4 and Ha= 0 isotharms have more curves, this indicates more powerful natural convection of nanofluid. At this Rayleigh and with increasing Hartmann number, isotherms is similar to its status at Ra =10^3 that shows thermal conduction domination compared with behavior of nanofluid. In Ra=10^5, isotherms have before curve attain to Ha=50. That because the inflence of Lorentz force at this Hartmann=50 is not high adequately to prevent natural convection of nanofluid and cause conduction dominate. For Ra =10^5 and Ha =100 the Lorentz force is high enough to prevent natural convection of nanofluid and cause isotherms be similar to isotherms at Rayleigh(=10^3,10^4). Total entropy lines are more densely packed adjacent the bottom vertices of the enclosure for Rayleigh number (=10^3,10^4). In thease regions, isotherms are denser,too. That indicates more temperature gradient in these regions. At next sections it will be shown that main contribution of total entropy is generated entropy due to heat transfer, consequently, total entropy lines are more densely packed at this regions. This behavior is observed for all investigated Rayleigh and Hartmann numbers, except for Ra=10^5 and Ha =0. For Ra =10^5 and Ha=0, because natural convection is dominant and causes entropy generation due to friction to have more contribution and also leads to more heat transfer, total entropy lines are observed adjascent of the cold walls and large portion of bottom hot wall. Total entropy are denser at this regions that indicates more entropy generation.Tables 5 and 6, show amounts of $|\psi_{max}|$ as the criterion of the flow power at different Hartmann numbers and volume fractions for Rayleigh numbers (10^3-10^5). At Ra =10^3 and for all investigated Hartmann numbers, $|\psi_{max}|$ decreases with increasing the volume fraction of nanoparticles. Because of low movement of nanofluid at Ra=10^3, with increasing the viscosity of nanofluid affected enhancement of volume fraction of nanoparticles, nanofluid motion be prevented and consequently, $|\psi_{max}|$ decreased. Also it is observed that for Ra=10^4 natural convection of nanofluid is insignificant because of the low amount of Rayleigh number like Ra=10^3, so with increasing the volume fraction of nanofluid $|\psi_{max}|$ has similar behavior.

Table 5
Amounts of $|\psi_{max}|$ at different Ha and volume fractions for Ra=10^3.

ψ	Ha=0	Ha=50	Ha=100
0	0.1253	0.0151	0.0049
0.02	0.1117	0.0140	0.0045
0.04	0.1005	0.0129	0.0042

Table 6
Amounts of $|\psi_{max}|$ at different Hartmann numbers and volume fractions for Ra=10^4.

ψ	Ha=0	Ha=50	Ha=100
0	2.9191	0.1607	0.0498
0.02	2.5068	0.1463	0.0459
0.04	2.0417	0.1341	0.0425

Table 7 shows amounts of $|\psi_{max}|$ at different Hartmann numbers and volume fractions for Ra=10^5. At Rayleigh =10^5 unlike the Rayleigh numbers (=10^3,10^4), $|\psi_{max}|$ increases with increasing volume fraction of nanoparticles for Hartmann=0.

By enhancement of volume fraction of nanoparticles, thermal conductivity coefficient and viscosity of nanofluid increase. Increment of the thermal conductivity coefficient cause appropriate heat transfer and consequently enhanced convection. Whereas, increase of the viscosity prevent from suitable convection.At this Rayleigh number and for Ha=0, the increasing effect of the thermal conductivity coefficient on natural convection dominates on the decreasing effect of thermal viscosity. For Ra=10^5 and Ha=50,100 influence of increasing volume fraction on $|\psi_{max}|$ is similar to Ra=10^3,10^4, because the Lorentz force due to magnetic field weakens natural convection of nanofluid.

For all investigated Rayleigh numbers, Hartmann numbers and volume fractions, maximum value of $|\psi_{max}|$ is 16.3 and occurs for Ra=10^5, volume $|\psi_{max}|$ is 16.3 and occurs for Ra=10^5, volume fraction=0.04.

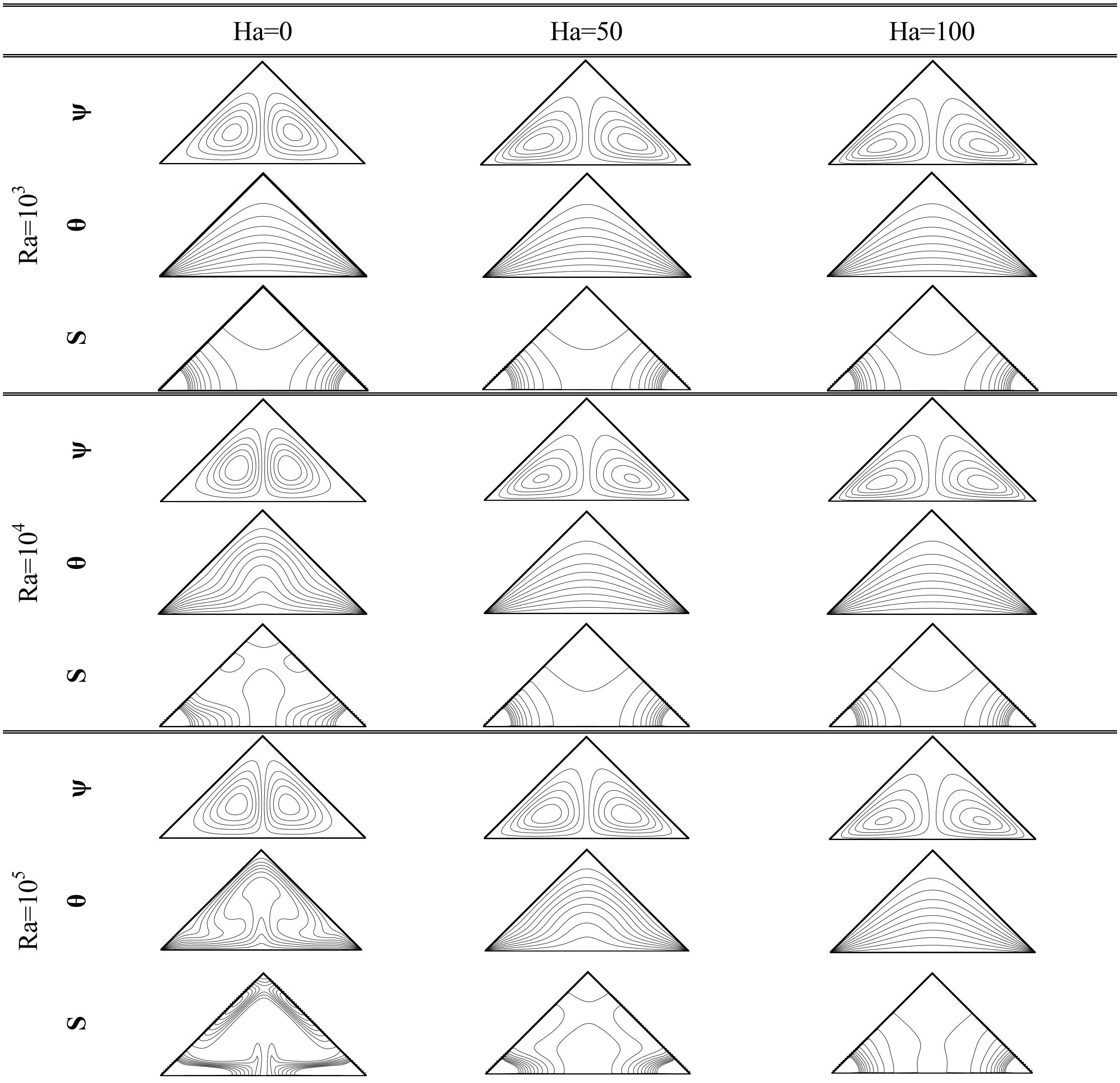

Fig. 2. Streamlines, isotherms and total entropy at different Rayleigh and Hartmann numbers

Whereas minimum value of $|\psi_{max}|$ is 0.1005 and occur for Ra=10^3 and φ=0.04.

Table 7
Amounts of $|\psi_{max}|$ at different Hartmann numbers and volume fractions for Ra=10^5.

ψ	Ha=0	Ha=50	Ha=100
0	15.5098	2.7777	0.5898
0.02	16.0280	2.4052	0.5223
0.04	16.3008	2.0410	0.4702

The variations of average Nusselt number and total entropy generation with respect to the volume fraction for different Rayleigh and Hartmann numbers are shown in figure 3 For all investigated Rayleigh and Hartmann numbers, average Nusselt number increases with increasing the volume fraction of nanoparticles.

By increasing volume fraction of nanoparticles, thermal conductivity coefficient increases, so increment of the average Nusselt number is reasonable. Therefore, by enhancement of Hartmann number, the heat transfer regime is conduction-dominated. Subsequently, with increasing the Hartmann number, influence of Rayleigh number on motion of nanofluid becomes low. For Ha=50, the variations of Nusselt number in Ra= 10^3,10^4 are the same and this variation for Ra=10^5 is similar to two mentioned Rayleigh numbers. At Ha=100, the variation ranges of Nusselt number is the same for all Rayleigh numbers and lines coincide.

By enhancement of Hartmann, maximum decrease of average Nusselt number is 25.03% that occurs for Ra=10^5 and φ=0. Whereas, with increasing Hartmann number ,minimum decrease of average Nusselt number is 0.006 % occurs for Ra=10^4 and volume fraction of 0.04. As it can be observed from Fig.3, for investigated Rayleigh and Hartmann numbers, by enhancement of volume fraction of nanoparticles total entropy generation increases. Entropy generation is due to heat transfer and fluid friction. As it can be seen from tables 8-10 the amounts of entropy generation due to friction are insignificant and main contribution of entropy generation is due to heat transfer.

Consequently, the variation of total entropy should be similar to variation of average Nusselt number with increasing the volume fraction. The maximum value of total entropy generation is 33.16 and occurs for Ra=10^5, Ha=0 and φ=0. Whereas the minimum value of total entropy generation is 19.73 which occurs at Ra=10^3, Ha=100 and φ=0.

As it observed from tables 8-11 with increasing the volume fraction for all investigated Rayleigh and Hartmann numbers, the contribution of entropy generation due to friction become less, because heat transfer increases by enhancement of volume fraction and, subsequently, the contribution of entropy generation due to heat transfer is more. However, as mentioned before, behavior of $|\psi_{max}|$ at Ra=10^5 and Ha=0 variations of entropy generation due to heat transfer is inverse of other situations. Because at Ra=10^5 and Ha=0, $|\psi_{max}|$ increases with increasing the volume fraction, consequently entropy generation due to friction become more, too.

Table 8
Entropy generation due to friction for different volume fractions and Hartmann numbers at Ra=10^3.

ψ	Ha=0	Ha=50	Ha=100
0	4.87E-03	2.24E-04	4.21E-05
0.02	4.21E-03	2.04E-04	3.85E-05
0.04	3.69E-03	1.87E-04	3.54E-05

Table 9
Entropy generation due to friction for different volume fractions and Hartmann numbers at Ra=10^4.

ψ	Ha=0	Ha=50	Ha=100
0	2.09×10^{-2}	2.42×10^{-4}	4.29×10^{-5}
0.02	1.66×10^{-2}	2.17×10^{-4}	3.91×10^{-5}
0.04	1.20×10^{-2}	1.96×10^{-4}	3.58×10^{-5}

Table 10
Entropy generation due to friction for different volume fractions and Hartmann numbers at Ra=10^5.

ψ	Ha=0	Ha=50	Ha=100
0	8.76×10-3	5.13×10-4	5.29×10-5
0.02	9.24×10-3	4.18×10-4	4.58×10-5
0.04	9.56×10-3	3.37×10-4	4.05×10-5

5. Conclusion

At present study the mixed convection flow, heat transfer and entropy generation of Al_2o_3-Water nanofluid with various properties affected by magnetic field in triangular enclosure was investigated. Side walls of the enclosure are cold and bottom wall is hot. This study is carried out for Ra=10^3,10^4,10^5, Ha=0, 50,100, angle of inclined sidewalls =45° and volume fraction of nanoparticle=0-0.04. Numerical results show that:

1. with applying and increasing the magnetic field (enhancement of Hartmann number) velocity of nanofluid and, subsequently, stream function magnitude in enclosure decreases because of the Lorentz force.

2. With increasing the Hartmann number, natural convection becomes weak and heat transfer regime is conduction-dominated.

3. for all investigated Rayleigh and Hartmann numbers and volume fractions, maximum absolute value $|\psi_{max}|$ is 16.3 that occurs at Ra=10^5 and φ=0.04. Whereas the minimum absolute value of $|\Psi|_{max}$ is 0.1005 occurs for Ra=10^3 and φ=0.04.

4. For all investigated Rayleigh and Hartmann numbers, average Nusselt number increases with increasing the volume fraction of nanoparticles.

5. Maximum decrease of average Nusselt number is 25.03% that occurs for Ra=10^5 and φ=0 with increasing the Hartmann number. Whereas, minimum decrease of average Nusselt number is 0.006% occur for Ra=10^4 and φ=0.04 with increasing the Hartmann number.

6. For all investigated Rayleigh and Hartmann number, total entropy generation increases by enhancement of volume fraction of nanoparticles.

7. Value of the maximum total entropy generation is 33.16 that occurs for Ra=10^5, Ha=0 and φ=0. Whereas,

The amount of the minimum total entropy generation is 19.73 that occurs for Ra=10^3, Ha=100 and φ=0.

8. In all investigated situations, total entropy generation due to friction is insignificant and main contribution of entropy generation is due to heat transfer. So, the variations of total entropy generation is similar to variation of average Nusselt number.

References

[1] B. Ghasemi, S.M. Aminossadati, Mixed convection in a lid-driven triangular enclosure filled with nanofluids, Int. Commun. in Heat Mass Transfer 37 (2010) 1142–1148.

[2] CJ. Ho, MW. Chen, ZW. Li, Numerical simulation of natural convection of nanofluid in a square enclosure: effects due to uncertainties of viscosity and thermal conductivity, Int. J. Heat Mass Transfer 51 (2008) 4506–4516.

[3] H. Oztop, E. Abu-Nada, Numerical study of natural convection in partially heated rectangular enclosures filled with nanofluids, Int. J. Heat Fluid Flow, 29, (2008),1326–1336.

[4] M. Mahmoodi, S.S. Hashemi, Numerical study of natural convection of a nanofluid in C-shaped enclosures, Int. J. Thermal Sciences 55 (2012) 76-89.

[5] A. Bejan, Second law analysis in heat transfer, Energy 5 (1980) 721-732.

[6] O. Mahian, S. Mahmud, I. Pop, Analysis of first and second laws of thermodynamics between two isothermal cylinders with relative rotation in the presence of MHD flow, Int. J. Heat Mass Transfer 55 (2012) 4808-4816.

[7] E. Dagtekin, H.F. Oztop, A. Bahloul, Entropy generation for natural convection in Γ-shaped enclosures, Int. Commun. Heat Mass Transfer 34 (2007) 502–510.

[8] G.G. Ilis, M. Mobedi, B. Sunden, Effect of aspect ratio on entropy generation in a rectangular cavity with differentially heated vertical walls, Int. Commun. Heat Mass Transfer 35(2008) 696–703.

[9] Y. Varol, H.F. Oztop, A. Koca, Entropy generation due to conjugate natural convection in enclosures bounded by vertical solid walls with different thicknesses, Int. Commun. Heat Mass Transfer 35 (2008) 648–656.

[10] A. A. Abbasian Arani, J. Amani, Experimental study on the effect of TiO2–water nanofluid on heat transfer and pressure drop, Experiment. Thermal Fluid Science 42 (2012) 107-115.

[11] A. A. Abbasian Arani, J. Amani, Experimental investigation of diameter effect on heat transfer performance and pressure drop of TiO2–water nanofluid, Experiment. Thermal Fluid Science 44 (2013) 520-533.

[12] E. Abu-Nada, Z. Masoud, A. Hijazi, Natural convection heat transfer enhancement in horizontal concentric annuli using nanofluids, Int. Commun. Heat Mass Transfer 35(2008) 657–665.

[13] A. Bejan, Entropy Generation Minimization, CRC Press New York (1995).

[14] H.C. Brinkman, The viscosity of concentrated suspensions and solution", J. Chemical Physics 20 (1952) 571–581.

[15] J.C. Maxwell-Garnett, Colours in metal glasses and in metallic films, Philos, Trans. Roy. Soc. A 203 (1904) 385-420.

[16] J. Koo, C. Kleinstreuer, a new thermal conductivity model for nanofluids", J.Nanoparticle Research 6 (2004) 577–588.

[17] J. Li, C. Kleinstreuer, Thermal performance of nanofluid flow in microchannels, Int. J. Heat Fluid Flow 29 (2008) 1221–1232